IJIREEICE ISSN (O) 2321-2004, ISSN (P) 2321-5526

International Journal of Innovative Research in Electrical, Electronics, Instrumentation and Control Engineering

Impact Factor 8.414 ⁜ Peer-reviewed & Refereed journal ⁜ Vol. 14, Issue 10, October 2026

Smart Transformer Health Monitoring System Using Multi-Parameter Sensing and Early Anomaly Detection

Agnivo Chowdhury[1], Saumya Pankaj Kumar[2], Jatin Satapathy[3], Ayan Saikia[4],

Hareesh Dash[5], Karthikeya Bhandari[6], A. Thamilamaran[7]

School of Electrical Engineering, Vellore Institute of Technology, Vellore, India[1,2,3,4,5,6]

Faculty Guide, School of Electrical Engineering, Vellore Institute of Technology, Vellore, India[7]

Abstract: This paper presents a low-cost, non-invasive health monitoring system for transformers. Conventional protection relies on static, per-parameter alarm limits that react only after a quantity is already dangerously high, while commercial diagnostic equipment is expensive. The prototype is built around an Arduino Uno that measures voltage, current and surface temperature using a 0–25 V voltage-sensor module, ACS712 Hall-effect current sensors and an analog temperature sensor, and displays the readings on a 16×2 LCD. Beyond display, the measurements are interpreted jointly: a baseline operating signature relating temperature, vibration and voltage to load current is established, and the normalized deviations from it are fused into one anomaly score and a 0–100 health index. A simulation framework (first-order thermal model, I^2 vibration model, sensor noise and ADC quantization) is used to compare this approach with conventional threshold alarms. Over 300 Monte-Carlo runs per scenario, the fusion method confirmed a developing cooling fault 19.5 min after onset against 39.5 min for static thresholds, detected a developing mechanical fault that the thresholds missed in 100% of runs, and raised no false anomaly alarm during a load-explained overload. The work provides the foundation for experimental validation, machine-learning and edge-based extensions.

Index Terms: Transformer condition monitoring, sensor fusion, anomaly detection, Arduino, ACS712, health index, measurement and instrumentation.

I. Introduction

Power and distribution transformers are among the most expensive and critical assets of an electrical network, and their unplanned failure causes outages and costly repairs. The life of a transformer is governed largely by the thermal ageing of its insulation, which depends on loading and on how well heat is removed [1, 2]. Established condition-assessment techniques such as dissolved-gas analysis [3] and vibration analysis [4, 5] give deep insight, but they need specialised sensors and instruments that are out of reach for small installations and teaching laboratories.

In practice, transformers are monitored by periodic manual inspection or by static alarm limits on individual quantities, for example "temperature > limit". Manual inspection gives no continuous record. Static limits react only after a parameter is already high, and they cannot tell heating that is *explained* by a high load from heating caused by a developing defect. A useful monitor should therefore read several quantities together and judge whether their *relationship* is still normal.

Inexpensive microcontroller boards with built-in analog-to-digital converters (ADCs) make multi-channel acquisition affordable [10, 9], and mechanical and electrical quantities can be read without opening the transformer. Measurement quality, however, depends on calibration, resolution and noise, which must be analysed explicitly [9, 15, 16].

This paper reports a Measurements and Instrumentation project with the following contributions:

- a low-cost, non-invasive prototype measuring voltage, current and temperature with an Arduino Uno and a local LCD display;
- a baseline-signature and residual-based sensor-fusion algorithm producing an anomaly score, a health index and a Normal/Watch/Abnormal status;
- a documented simulation framework comparing the algorithm with static thresholds, including detection delay, false alarms and ROC analysis; and
- a roadmap towards machine learning, edge processing and remaining-useful-life estimation.

The research question guiding the work is: *can low-cost multi-parameter sensing and sensor fusion detect early transformer anomalies before conventional threshold-based protection is triggered?*

II. Monitoring Approaches and Related Work

Transformer monitoring can be grouped into three levels (Table I). Level 1 is periodic manual checking. Level 2 is online monitoring, where sensors measure voltage, current, temperature and sometimes vibration or humidity and send

the data to a display or remote dashboard; microcontroller-based dashboards of this kind are common, so connectivity alone is not a novelty. Level 3 is intelligent condition monitoring, where the system reports that the *operating pattern* deviates from the normal baseline, instead of that a value has crossed a limit. The present work targets Level 3 using low-cost hardware.

TABLE I. MONITORING APPROACHES COMPARED

Level	Decision logic	Main limitation
1 Manual	Technician judgement at periodic visits	No continuous record
2 Online	Static limit on each parameter (e.g. $T > T_{lim}$)	Late warning; load-driven false alarms
3 Intelligent (this work)	Deviation of the *V–I–T–* vibration *relationship* from a baseline signature	Needs baseline data; hardware validation pending

Two physical relationships underpin the approach. First, the winding (copper) loss grows with the square of the load current, and the temperature follows through a thermal time constant; dynamic thermal models of this form are widely used [7, 1]. Second, tank vibration is caused by the core (magnetostriction, mainly $\propto V^2$) and by winding forces ($\propto I^2$), with the dominant component at twice the supply frequency [5, 6]. Because both effects depend on load, a deviation from the expected temperature or vibration *at the present load* is a more sensitive indicator than any fixed limit. Detecting such deviations is an anomaly-detection problem [8].

III. SYSTEM ARCHITECTURE AND MEASUREMENT PRINCIPLES

A. Architecture

The system (Fig. 1) has five functional blocks: the transformer under test, the sensors, signal conditioning, the Arduino-based acquisition and processing unit, and the output (LCD and serial log). All sensors are mounted externally, so the transformer is not opened.

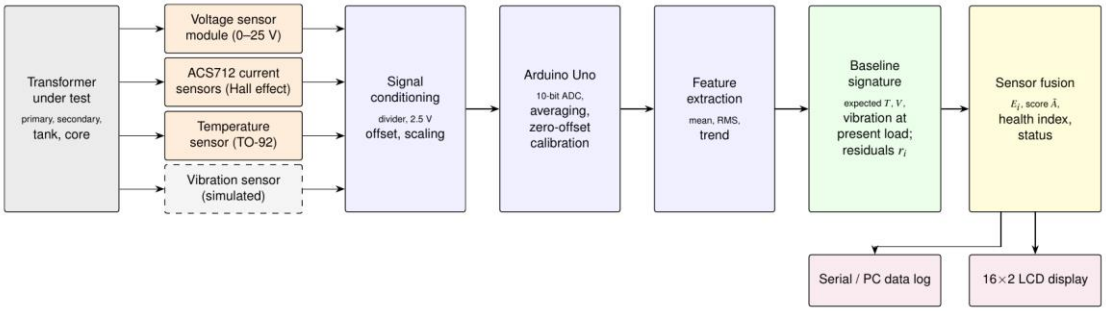


Fig. 1. Block diagram of the proposed transformer health monitoring system. Solid sensor blocks are in the hardware prototype; the vibration channel (dashed) is evaluated in simulation.

B. Measurement Equations

The ATmega328P ADC is 10-bit with a 5 V reference [13], so a count *N* corresponds to

$$V_{adc} = \frac{N}{1023} V_{ref}, \qquad V_{ref} = 5\ V. \tag{1}$$

Current: the ACS712 is a Hall-effect sensor whose output is centred at $V_{cc}/2$ and is linear in the primary current [11, 14]; for the 5 A variant (sensitivity $S = 0.185$ V/A),

$$I = \frac{V_{adc} - 2.5}{S}. \tag{2}$$

For alternating current, the RMS value over *M* samples covering whole mains cycles is

$$I_{rms} = \sqrt{\frac{1}{M}\sum_{k=1}^{M} (i_k - \bar{i})^2}. \tag{3}$$

Voltage: the 0–25 V module is a 5:1 resistive divider, so

$$V_{in} = \frac{R_1 + R_2}{R_2} V_{adc} = 5\, V_{adc}. \tag{4}$$

Temperature: the TO-92 analog sensor, an LM35-class device with 10 mV/°C output [12], gives

$$T = \frac{V_{adc}}{0.010}\ ^\circ C. \tag{5}$$

The per-channel signal chain is shown in Fig. 2. The voltage regulation of the transformer is

$$VR = \frac{V_{nl} - V_{fl}}{V_{fl}} \times 100\%, \qquad (6)$$

and the total loss, which drives the temperature rise, is

$$P = P_{fe} + I^2 R_{eq}, \qquad (7)$$

with P_{fe} the core loss and $I^2 R_{eq}$ the copper loss [17].

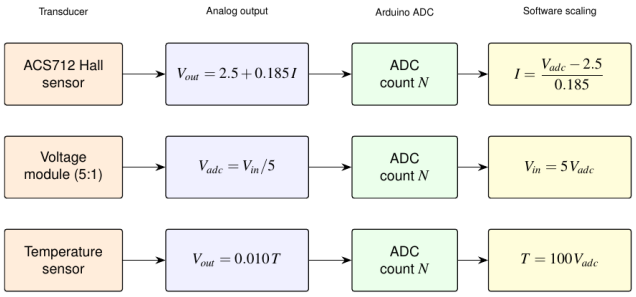


Fig. 2. Signal chain of the three measured channels, from transducer to engineering units.

IV. Hardware Implementation

A. Prototype

The hardware prototype (Fig. 3) is assembled on a breadboard mounted on a cardboard base. The Arduino Uno (1) is the acquisition and processing unit and is powered and read through a USB cable (7). The voltage-sensor module (2) and two ACS712 modules (3, 4) provide the electrical measurements, a TO-92 temperature sensor sits on the breadboard (6), and a 16×2 LCD (5) shows the readings locally. Table II lists the components.

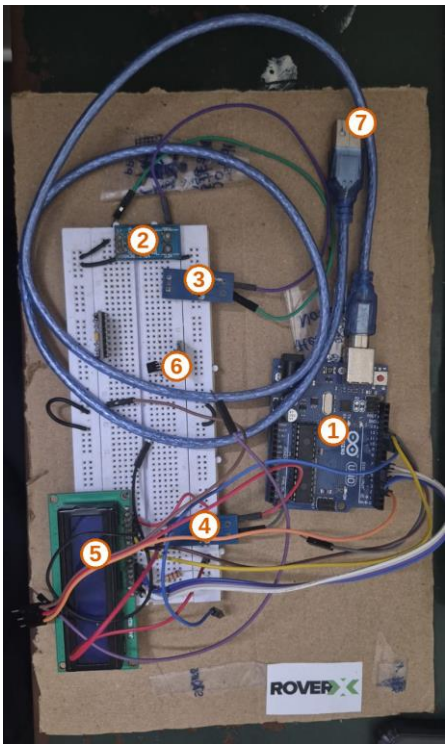


Fig. 3. Hardware prototype. (1) Arduino Uno, (2) 0–25 V voltage-sensor module, (3), (4) ACS712 current-sensor modules, (5) 16×2 LCD, (6) TO-92 temperature sensor on breadboard, (7) USB cable for power and serial communication.

TABLE II. HARDWARE COMPONENTS

Component	Qty	Role in the prototype
Arduino Uno (ATmega328P)	1	Acquisition, processing, display driver
ACS712 current sensor module	2	Hall-effect current measurement
Voltage-sensor module, 0–25 V	1	5:1 divider for voltage measurement
TO-92 analog temperature sensor	1	Surface temperature
16×2 character LCD	1	Local display
Resistor, jumper wires, breadboard	–	Interconnection
USB cable	1	5 V power and serial link

B. Resolution and Measurement Uncertainty

With a 5 V reference and 10-bit conversion, one ADC step corresponds to the values in Table III. The ACS712 and the temperature sensor have the coarsest steps relative to their useful range, so current is the most resolution-limited channel for small loads (Fig. 4); averaging several samples and, for temperature, the 1.1 V internal reference (about 0.1 °C/LSB) are straightforward improvements. The percentage error of any channel against a reference instrument is

$$\varepsilon\,[\%] = \frac{|X_m - X_t|}{X_t} \times 100. \qquad (8)$$

TABLE III. CHANNEL SPECIFICATION AND RESOLUTION

Channel	Sensitivity	Range used	1 LSB
Current (ACS712-5A)	185 mV/A	±5 A	26.4 mA
Voltage (module)	$V_{in}/5$	0–25 V	24.4 mV
Temperature (LM35-class)	10 mV/°C	0–150 °C	0.49 °C

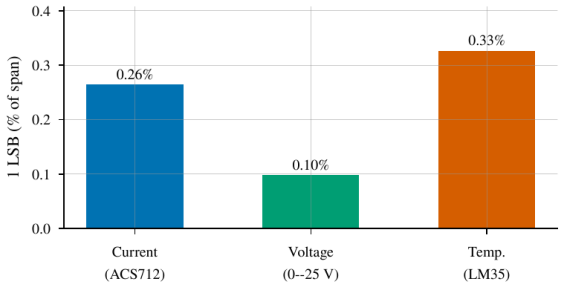


Fig. 4. Quantization step of each channel as a percentage of its span.

V. SOFTWARE AND HEALTH-ASSESSMENT ALGORITHM

A. Acquisition and Baseline Signature

The firmware initializes the ADC, LCD and serial port, determines the ACS712 zero-current offset, and then repeatedly reads each channel with averaging and converts it to engineering units (Fig. 5). Healthy dwell tests at several controlled load levels establish the *normal operating signature*: steady-state temperature and vibration are fitted against I^2, and secondary voltage against I,

$$T_{ss} = \alpha_T + \beta_T I^2, \quad a_{ss} = \alpha_a + \beta_a I^2, \quad V = V_0 - \gamma I. \quad (9)$$

The temperature at the present load is predicted with the first-order thermal lag

$$T_{exp}[k+1] = T_{exp}[k] + \left(1 - e^{-\Delta t/\tau}\right)\left(T_{ss}(I[k]) - T_{exp}[k]\right), \quad (10)$$

which follows from $C\,dT/dt = P - (T - T_a)/R_{th}$ with P from (7) and $\tau = R_{th}C$ [7].

IJIREEICE ISSN (O) 2321-2004, ISSN (P) 2321-5526

International Journal of Innovative Research in Electrical, Electronics, Instrumentation and Control Engineering

Impact Factor 8.414 ⁜ Peer-reviewed & Refereed journal ⁜ Vol. 14, Issue 10, October 2026

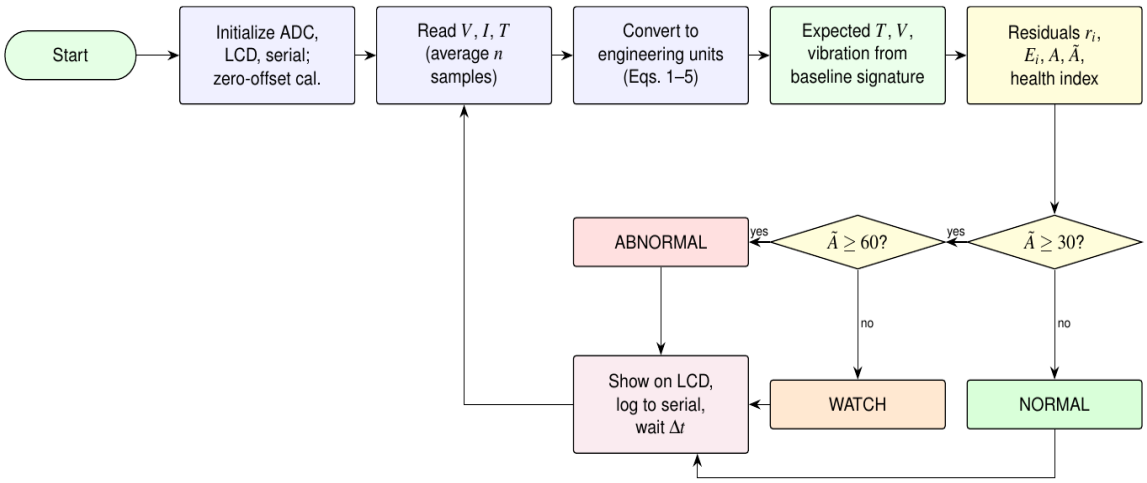


Fig. 5. Flowchart of the monitoring firmware and the health-assessment decision logic.

B. Residuals, Anomaly Score and Health Index

For each fused channel $i \in \{T, vib, V, I\}$ the residual r_i is the measured value minus its expected value at the present load; for the current channel it is the difference between the two ACS712 readings, which acts as a sensor-consistency check. The normalized deviation uses a dead-band $\delta_i = 0.25\, r_{max,i}$ to ignore noise:

$$E_i = min\left(1, max\left(0, \frac{|r_i| - \delta_i}{r_{max,i} - \delta_i}\right)\right). \qquad (11)$$

The instantaneous anomaly score, its exponentially weighted smoothing and the health index are

$$A = 100 \sum_i \quad w_i E_i, \qquad HI = 100 - \tilde{A}, \qquad (12)$$

$$\tilde{A}[k] = \lambda A[k] + (1 - \lambda)\tilde{A}[k-1], \qquad (13)$$

with the weights, scales and limits of Table IV. A status is declared only after three consecutive samples satisfy a condition, which suppresses isolated noise.

TABLE IV. DETECTOR SETTINGS AND STATIC LIMITS

Channel	w_i	$r_{max,i}$	Static limit
Temperature	0.40	6 °C	>65 °C
Vibration	0.30	0.04 g	>0.15 g
Voltage	0.20	0.5 V	<11.0 V
Current (consistency)	0.10	0.15 A	$> 1.10\, I_{rated}$

Note: $\lambda = 0.3$. Status: Normal $\tilde{A} < 30$; Watch $30 \leq \tilde{A} < 60$; Abnormal $\tilde{A} \geq 60$. Overload is reported separately when $I > 1.10\, I_{rated}$.

VI. SIMULATION FRAMEWORK

Because the hardware cannot yet be driven through controlled fault conditions, a simulation model was built to develop and test the algorithm before experimental validation. A 12 V, 1 A (12 VA-class) transformer is modelled with the parameters of Table V: temperature from the first-order thermal model above, vibration $a = a_0 + k_w I^2$ [5], and secondary voltage $V = V_{nl}(1 - VR \cdot I/I_r)$. Gaussian sensor noise and the ADC quantization steps of Table III are added. The baseline signature is re-identified in every run from simulated healthy dwell tests, so model-fit error is included. Four scenarios are run for 90 min, sampled every 10 s, with load stepping 25%, 50%, 75% at 0, 15 and 30 min:

- **A**: healthy loading;
- **B**: 115% overload between 30 and 60 min (heating explained by load);
- **C**: cooling degradation, R_{th} rising by 55% over 25 min from $t = 45$ min;
- **D**: mechanical looseness, with k_w +80%, copper resistance +30% and regulation +1.5 points over 25 min from $t = 45$ min.

All results in the next section are simulated, not measured on the prototype.

TABLE V. SIMULATION PARAMETERS

V_{nl} = 12.6 V	I_{rated} = 1.0 A	VR = 6%
T_a = 28 °C	R_{th} = 20 °C/W	τ = 10 min
P_{fe} = 0.6 W	R_{eq} = 1.2 Ω	a_0 = 0.02 g, k_w = 0.08 g/A^2
σ_I = 15 mA	σ_V = 40 mV	σ_T = 0.35 °C, σ_a = 5 mg

VII. RESULTS AND DISCUSSION

A. Sensor Characteristics and Baseline Signature

Fig. 6 shows the datasheet transfer characteristics that the firmware inverts, together with the quantization step of each channel. Fig. 7 shows the simulated healthy dwell tests: temperature and vibration are linear in I^2 and voltage is linear in I, which is what makes load-aware expectation possible.

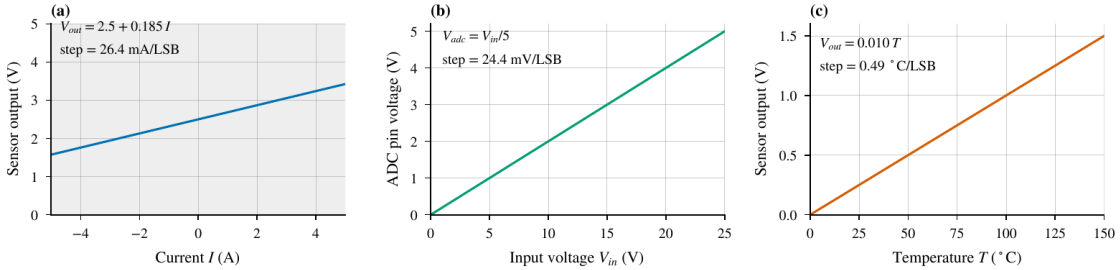


Fig. 6. Transfer characteristics of the three channels: (a) ACS712 (5 A), (b) voltage module, (c) analog temperature sensor.

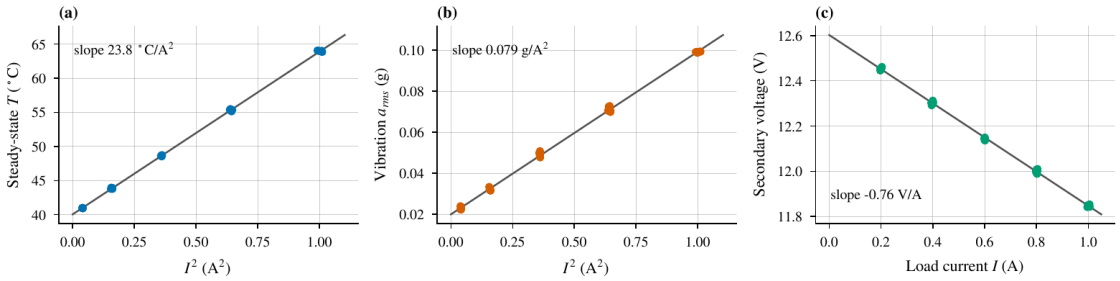


Fig. 7. Simulated normal operating signature from healthy dwell tests: (a) steady-state temperature versus I^2, (b) vibration versus I^2, (c) secondary voltage versus current, each with its least-squares fit.

B. Scenario Behaviour

In the cooling-degradation scenario (Fig. 8) the load is constant after 30 min, yet the measured temperature rises above the expected value after the fault starts at 45 min. The thermal residual reaches the Watch level well before the fixed 65 °C alarm is crossed, and the stacked contributions in panel (f) show that the temperature channel is responsible. In the mechanical scenario (Fig. 9) the vibration never reaches its static limit of 0.15 g, but both its residual and the thermal residual grow, so the health index falls steadily and the status moves from Normal to Watch and towards Abnormal because two channels deviate at once. During the 115% overload (Fig. 10) the temperature exceeds 65 °C and the static alarm is active for 100% of the overload window, but the measured temperature stays on its load-expected curve and the anomaly score remains below the Watch level (0% of the window flagged); the overload itself is reported by the separate current rule.

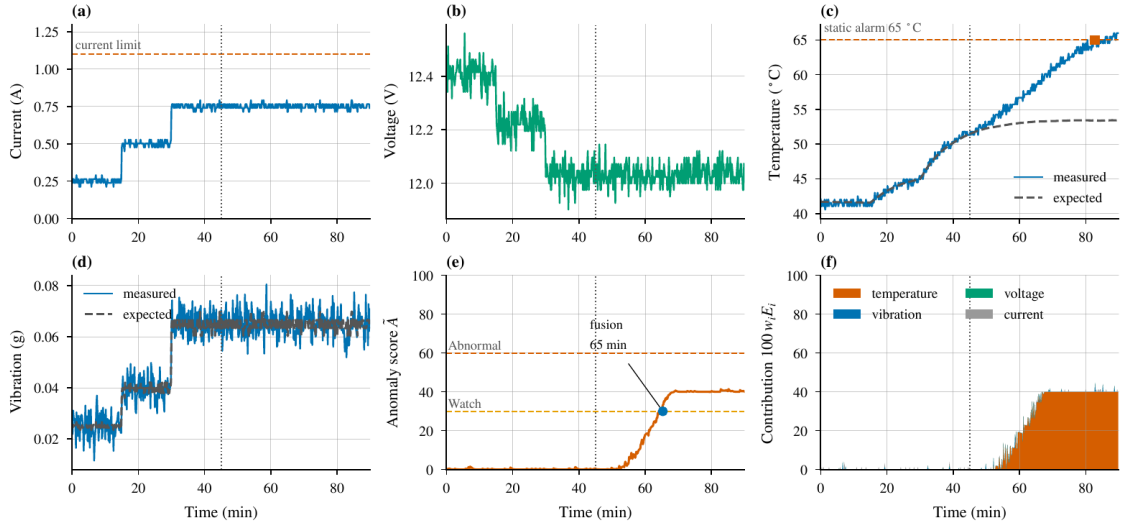


Fig. 8. Simulated scenario C (cooling degradation, onset at 45 min, dotted line): (a) current, (b) voltage, (c) temperature measured versus expected, with the static alarm marked as a square, (d) vibration, (e) anomaly score with Watch/Abnormal levels and fusion detection point, (f) contribution of each channel to the score.

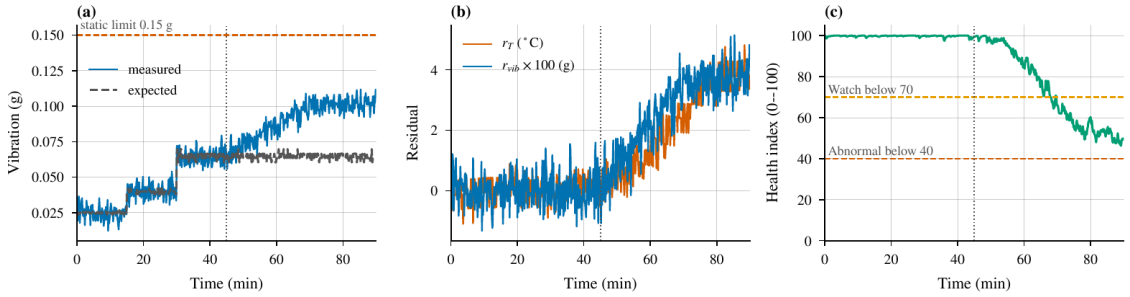


Fig. 9. Simulated scenario D (mechanical looseness): (a) vibration against its expected value and static limit, (b) residuals of temperature and vibration, (c) health index with status levels.

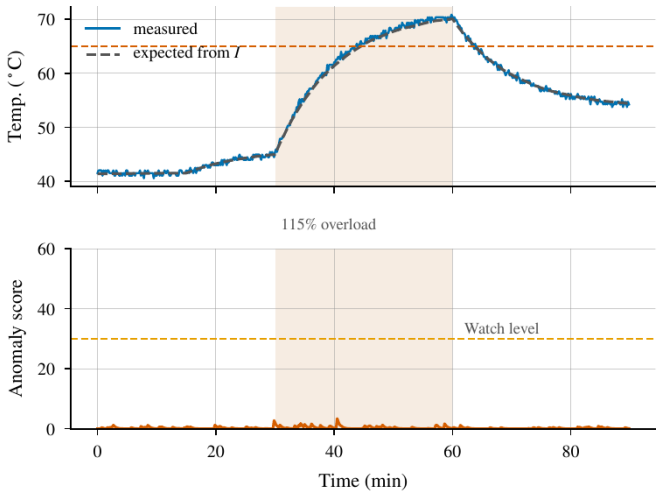


Fig. 10. Simulated scenario B: heating during the 115% overload is explained by the load, so the temperature stays on its expected curve and the anomaly score remains low.

C. Sensitivity, Correlation and Detection Performance

The score map of Fig. 11 shows that the score is near zero in healthy operation at every load and rises only with fault severity, which is the desired load-independent behaviour. A cooling fault alone saturates at 40 points (the temperature weight), so it yields Watch; the combined mechanical fault pushes the score towards, and at high load and severity above, the Abnormal level because several channels contribute. The correlation matrices of Fig. 12 show that current, voltage, temperature and vibration are all strongly correlated in both a healthy and a faulty run, simply because they follow the

common load profile. Raw correlation therefore cannot reveal the fault, which is why the algorithm works on residuals relative to the load-based expectation instead.

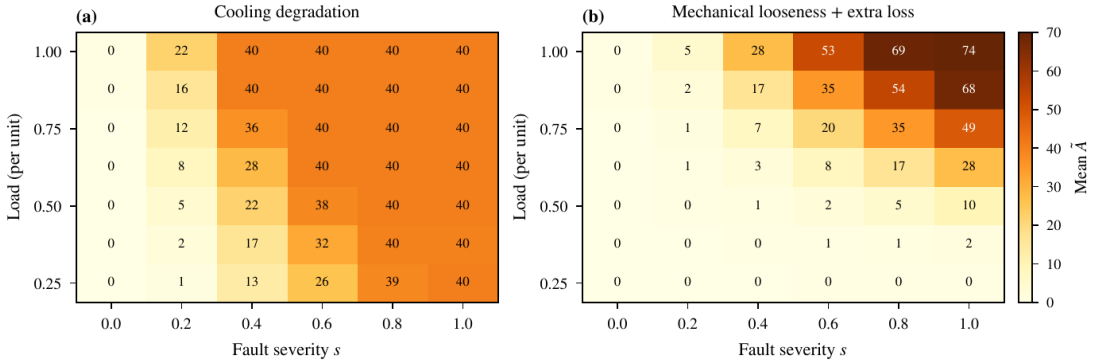


Fig. 11. Simulated steady-state mean anomaly score as a function of load and fault severity s for (a) cooling degradation and (b) mechanical looseness with extra loss.

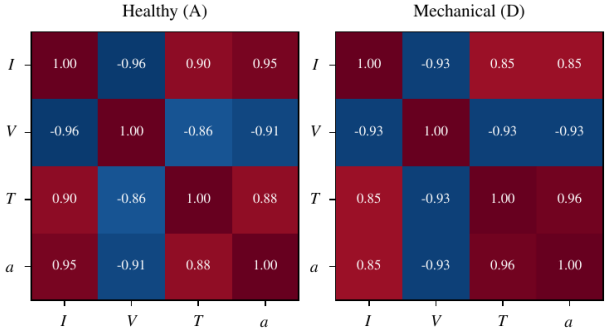


Fig. 12. Simulated correlation coefficients among current (I), voltage (V), temperature (T) and vibration (a) for a healthy run (A) and a mechanical-fault run (D); all follow the load.

Table VI and Figs. 13 and 14 summarize 300 Monte-Carlo runs per scenario (new noise and a new baseline identification each run). Detection delay is measured from fault onset to the first confirmed alarm. Fusion confirmed the cooling fault after 19.5 ± 0.4 min against 39.5 ± 0.9 min for the static limits, which is the earliest the conventional method can act because the temperature must physically reach 65 °C. For the mechanical fault the static limits detected nothing within 90 min, while fusion detected it after 23.3 ± 0.8 min. Neither method produced false alarms in healthy operation. When samples of the overload scenario are counted as non-anomalous, because the heating is load-explained, the static limits give a false-positive rate of 12.3% at the cost of a true-positive rate of only 7.2%, whereas fusion gives 58.0% and 0.0%, and the area under the ROC curve rises from 0.799 to 0.969. These figures depend on the assumed fault models and static limits and must be confirmed experimentally.

TABLE VI. SIMULATED COMPARISON OF STATIC THRESHOLDS AND SENSOR FUSION

Metric	Threshold	Fusion
Delay, thermal fault C (min)	39.5 ± 0.9	19.5 ± 0.4
Delay, mechanical fault D (min)	not detected	23.3 ± 0.8
Missed within 90 min, C / D (%)	0 / 100	0 / 0
False alarms, healthy run A (% runs)	0.0	0.0
Overload window flagged anomalous (%)	100	0
ROC area under curve	0.799	0.969

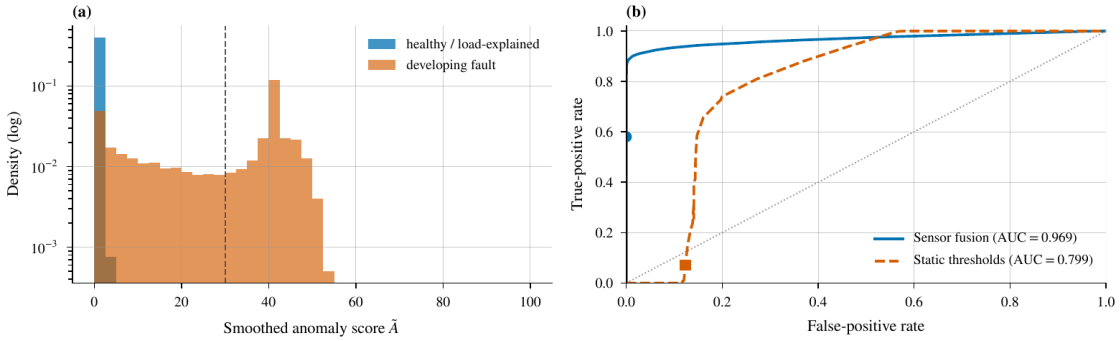


Fig. 13. (a) Distribution of the smoothed anomaly score for healthy/load-explained samples and for developing-fault samples. (b) ROC curves of sensor fusion and static thresholds; markers show the operating points of the alarm levels in Table IV.

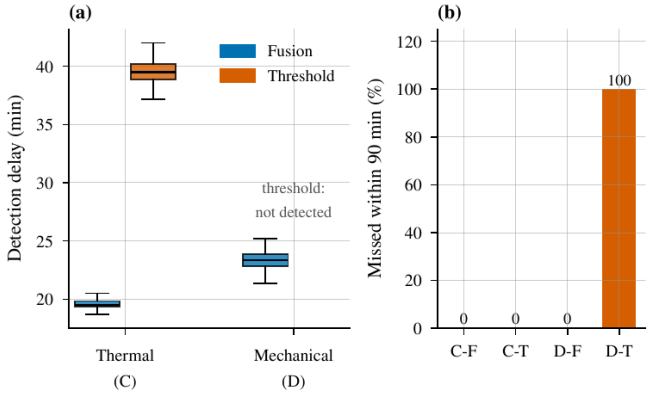


Fig. 14. (a) Detection delay of fusion (F) and threshold (T) methods for the thermal (C) and mechanical (D) faults. (b) Share of runs in which the fault was not detected within 90 min.

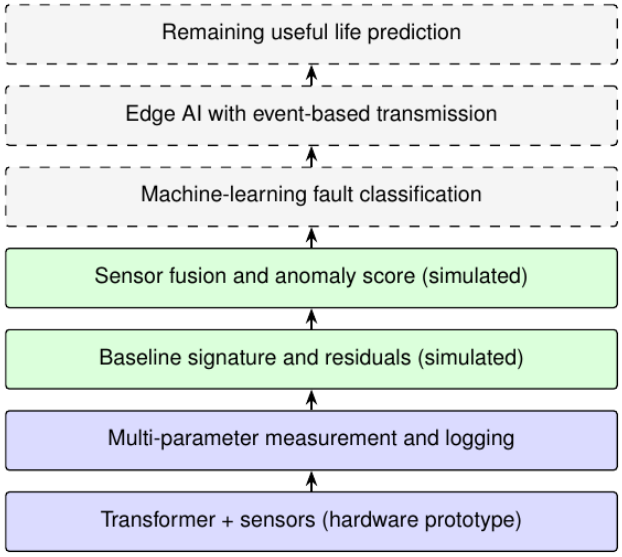


Fig. 15. Development roadmap. Filled blocks are implemented or simulated in this work; dashed blocks are future work.

VIII. Advantages Over Conventional Monitoring

- **Load-aware judgement:** temperature and vibration are judged against what the present load should produce, so load-driven heating is not mistaken for a defect, and a defect at moderate load is not hidden by a fixed limit.
- **Earlier warning:** deviations are flagged while every individual value is still below its static limit.
- **Low cost and non-invasive:** off-the-shelf modules on an Arduino Uno, with sensors mounted externally and no need to open the transformer.

- **Explainable output:** the stacked contributions show which channel causes the alarm, and the health index gives a single number for operators.
- **Data foundation:** every sample can be logged over serial, producing the experimental dataset needed for later machine-learning work.

IX. LIMITATIONS

(i) Results of Section VII are simulated; experimental validation on the prototype with controlled load tests and a calibrated reference meter is the next step. (ii) The 0–25 V voltage module is a DC divider; true AC RMS voltage needs a rectifier–filter stage or an AC sensing module. (iii) The 5 A ACS712 has a 26 mA step, which limits small-current accuracy, and the TO-92 sensor reads surface rather than winding temperature. (iv) Ambient temperature is assumed constant; a second temperature sensor would allow ambient compensation. (v) The vibration channel and the fault models are not yet validated on a real transformer, and the quoted limits are illustrative.

X. FUTURE SCOPE

The project is planned as a ladder (Fig. 15). After hardware validation of the baseline signature, the thresholds and weights will be tuned from real data; classifiers such as random forest, SVM or an autoencoder can then separate normal, overload, thermal and mechanical abnormalities. Processing on the microcontroller (edge analysis) with transmission of only significant events would reduce bandwidth for remote substations, and a health-index trend can support remaining-useful-life estimation. A candidate research title is “Low-Cost Multi-Parameter Sensor Fusion for Early Anomaly Detection in Distribution Transformers”; a conference-level claim requires experimental evidence of measurable advantage, including detection accuracy, false-alarm rate, detection time and measurement error against a reference.

XI. CONCLUSION

A low-cost Arduino-based transformer monitor measuring voltage, current and temperature was built, and a baseline-signature sensor-fusion algorithm was proposed and evaluated in simulation against static threshold alarms. In the simulated scenarios the fusion approach warned earlier of a thermal fault, detected a mechanical fault that fixed limits missed, and did not confuse a load-driven overload with a defect. The next steps are controlled load tests on the prototype, calibration against reference instruments, integration of the vibration channel, and data-driven extensions, so that the simulated advantage can be confirmed experimentally.

ACKNOWLEDGMENT

The authors thank the faculty guide for guidance during the Measurements and Instrumentation project.

REFERENCES

[1] *IEEE Guide for Loading Mineral-Oil-Immersed Transformers and Step-Voltage Regulators*, IEEE Std C57.91-2011, 2011.

[2] *Power Transformers—Part 7: Loading Guide for Mineral-Oil-Immersed Power Transformers*, IEC 60076-7, 2018.

[3] *IEEE Guide for the Interpretation of Gases Generated in Mineral Oil-Immersed Transformers*, IEEE Std C57.104-2019, 2019.

[4] M. Wang, A. J. Vandermaar, and K. D. Srivastava, “Review of condition assessment of power transformers in service,” *IEEE Elect. Insul. Mag.*, vol. 18, no. 6, pp. 12–25, Nov./Dec. 2002.

[5] B. García, J. C. Burgos, and A. M. Alonso, “Transformer tank vibration modeling as a method of detecting winding deformations—Part I: Theoretical foundation,” *IEEE Trans. Power Del.*, vol. 21, no. 1, pp. 157–163, Jan. 2006.

[6] B. García, J. C. Burgos, and A. M. Alonso, “Transformer tank vibration modeling as a method of detecting winding deformations—Part II: Experimental verification,” *IEEE Trans. Power Del.*, vol. 21, no. 1, pp. 164–169, Jan. 2006.

[7] D. Susa, M. Lehtonen, and H. Nordman, “Dynamic thermal modelling of power transformers,” *IEEE Trans. Power Del.*, vol. 20, no. 1, pp. 197–204, Jan. 2005.

[8] V. Chandola, A. Banerjee, and V. Kumar, “Anomaly detection: A survey,” *ACM Comput. Surv.*, vol. 41, no. 3, pp. 1–58, 2009.

[9] H. Y. Teh, A. W. Kempa-Liehr, and K. I-K. Wang, “Sensor data quality: A systematic review,” *J. Big Data*, vol. 7, no. 11, 2020.

[10] M. Simić, “Microcontroller-based readout of resistive sensors,” *IFAC-PapersOnLine*, vol. 55, no. 4, pp. 242–247, 2022.

[11] Allegro MicroSystems, “ACS712: Fully integrated, Hall effect-based linear current sensor IC,” datasheet.

[12] Texas Instruments, “LM35 precision centigrade temperature sensors,” datasheet.

[13] Microchip Technology, “ATmega328P 8-bit AVR microcontroller,” datasheet.

[14] E. Ramsden, *Hall-Effect Sensors: Theory and Application*, 2nd ed. Burlington, MA, USA: Newnes, 2006.

[15] J. P. Bentley, *Principles of Measurement Systems*, 4th ed. Harlow, U.K.: Pearson, 2005.

[16] A. S. Morris and R. Langari, *Measurement and Instrumentation: Theory and Application*. Oxford, U.K.: Academic Press, 2012.

[17] S. J. Chapman, *Electric Machinery Fundamentals*, 5th ed. New York, NY, USA: McGraw-Hill, 2012.